Application of Space-borne Radar Interferometry on Crustal Deformations in Taiwan

- A Perspective from the Nature of Events

Chung-Pai Chang*, Sin-Mei Ng and Jiun-Yee Yen
Center for Space and Remote Sensing Research, National Central University, Taiwan

Chi-Wen Lin
Central Geological Survey, MOEA, Taiwan

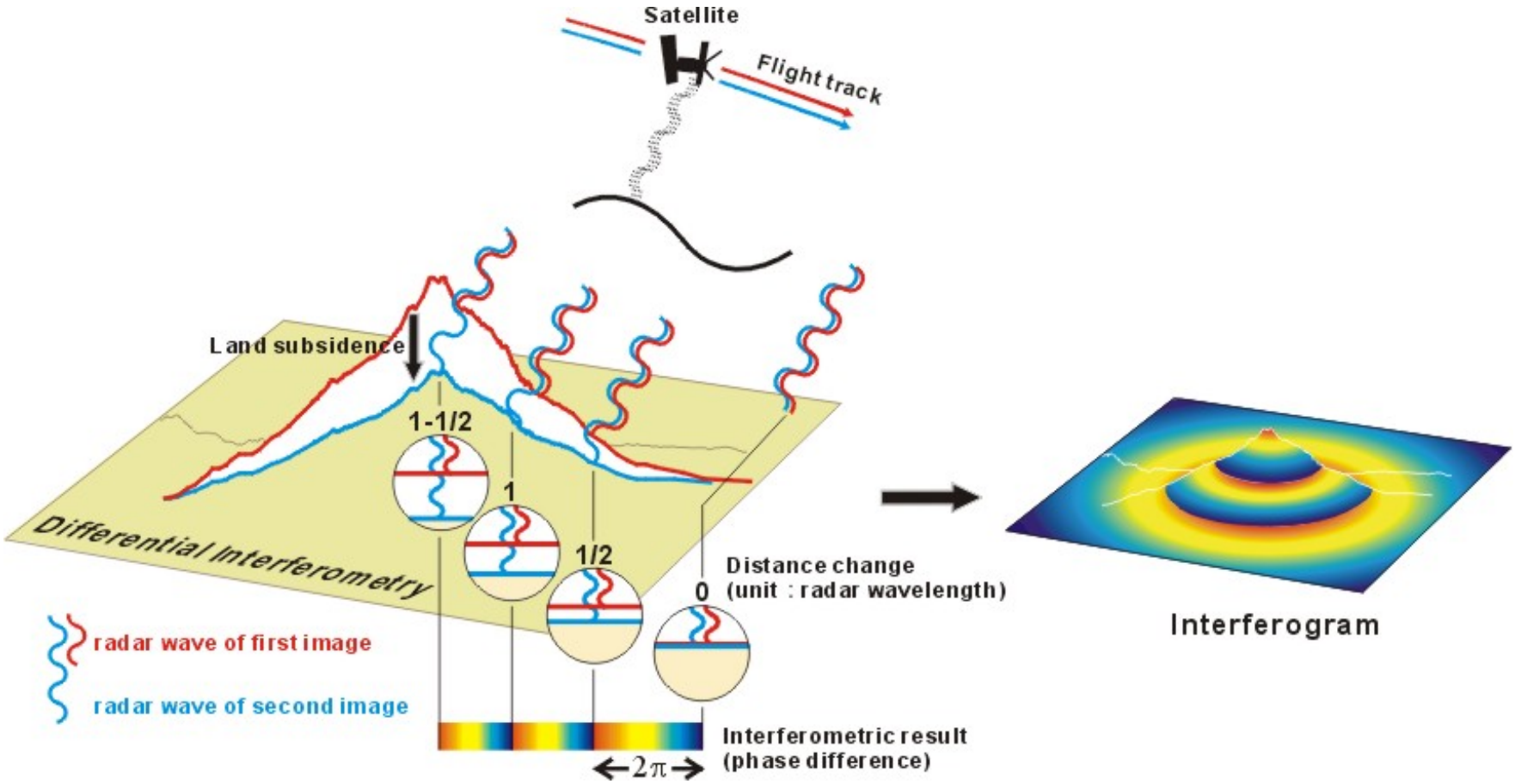

Schematic diagram showing how displacement fringes can be monitored using the interferometry techniques

The phase difference between two images acquired at different times creates an interference pattern called an interferogram. The interferogram shows the change in range from ground to satellite, that is, the component of the displacement vector of the surface that points toward the satellite.

Crustal deformation events of different nature

Nature of event	Intense	Gentle	Gentle
Cause of event	tectonic activity	tectonic activity	Human activity
Time scale of each event	days	Months~ years	Months~ years
Motion per incident	centimeters~ hundreds of centimenters	sub-centimeter	sub-centimeter
Recurring frequency	Year~ hundreds of years	daily (continuing)	daily (continuing)
Detectibility	easy	difficult	difficult
Example	Chichi coseismic deformation	Tainan and Hukou areas	Chungli and Pingtung areas

- Crustal deformations can be divided into two major categories based on duration of events and measures of ground offset, these being intense deformation and gentle deformation. There are various limitations when applying the radar interferometry technique to events of different type.

- The causes of gentle events include tectonic processes and human activities. These two effects may occur concurrently or compound each other creating a complex deformation pattern and making it difficult to attribute degrees of effect to each factor.

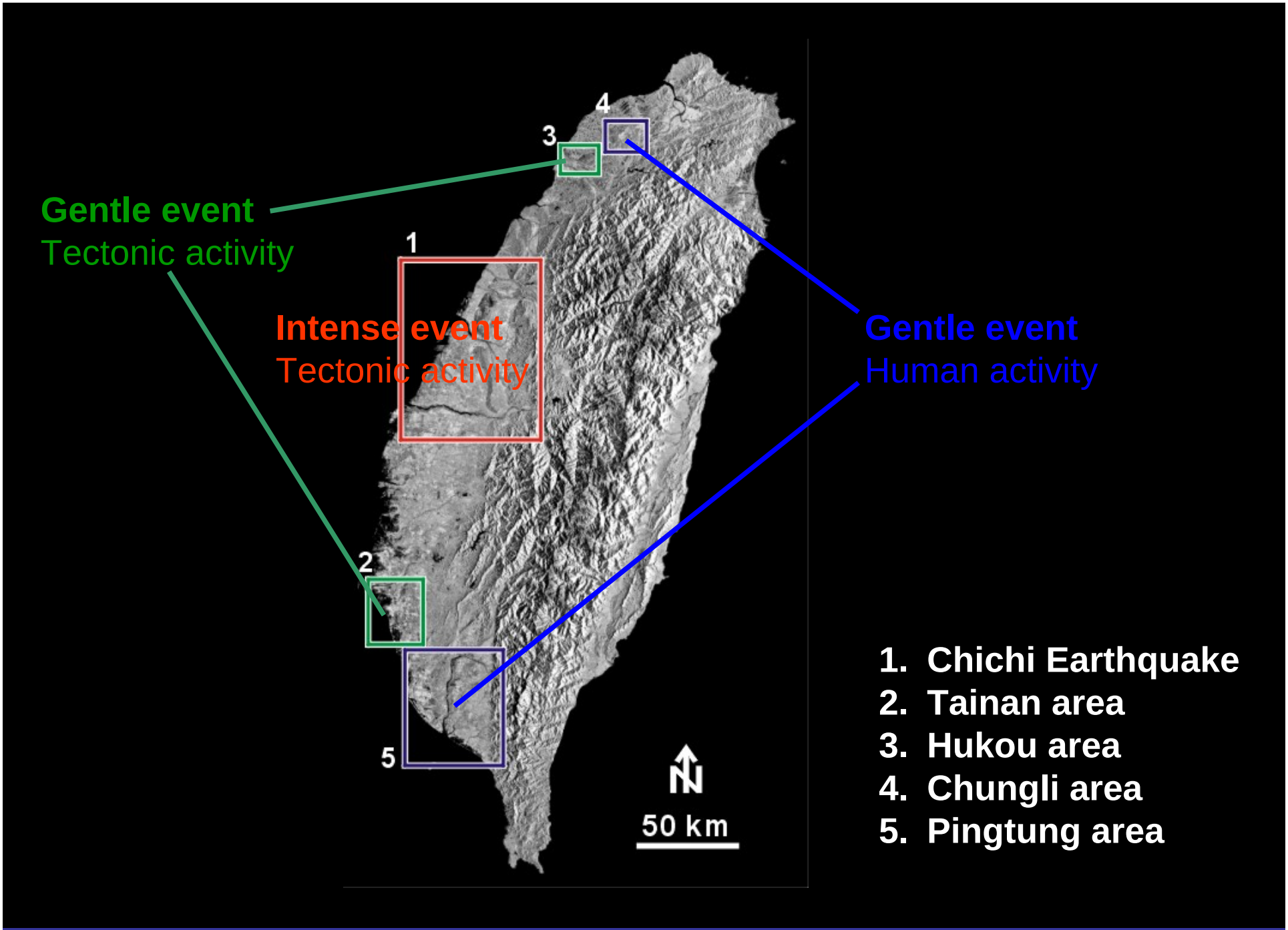
Gentle event
Tectonic activity
Intense event
Tectonic activity
Gentle event
Human activity
1
2
3
4
5
50 km
1. Chichi Earthquake
2. Tainan area
3. Hukou area
4. Chungli area
5. Pingtung area

1. Application of SAR interferometry to Chichi earthquake (central Taiwan)

Topographic map of the 1999 Chichi rupture (Chelungpu fault) and the neighboring major structures. The epicenter of the mainshock is shown as a red star. The focal mechanism of the mainshock by Central Weather Bureau are shown by equal area projection of the lower hemisphere.

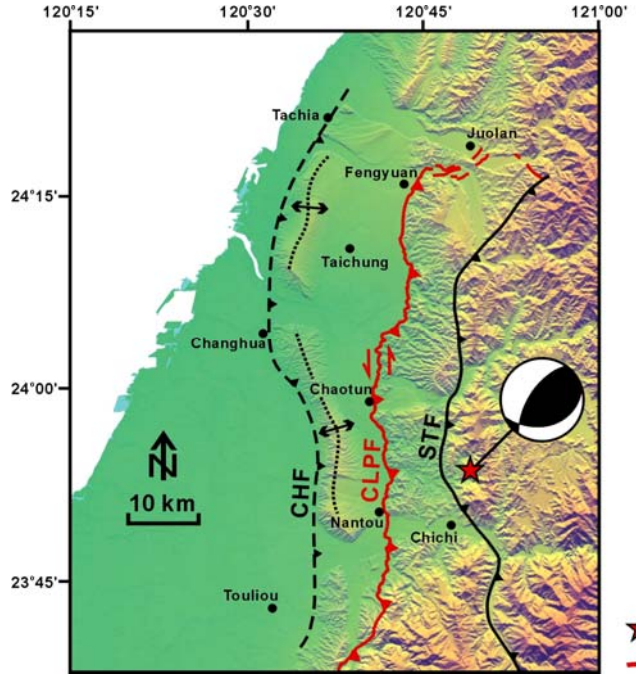

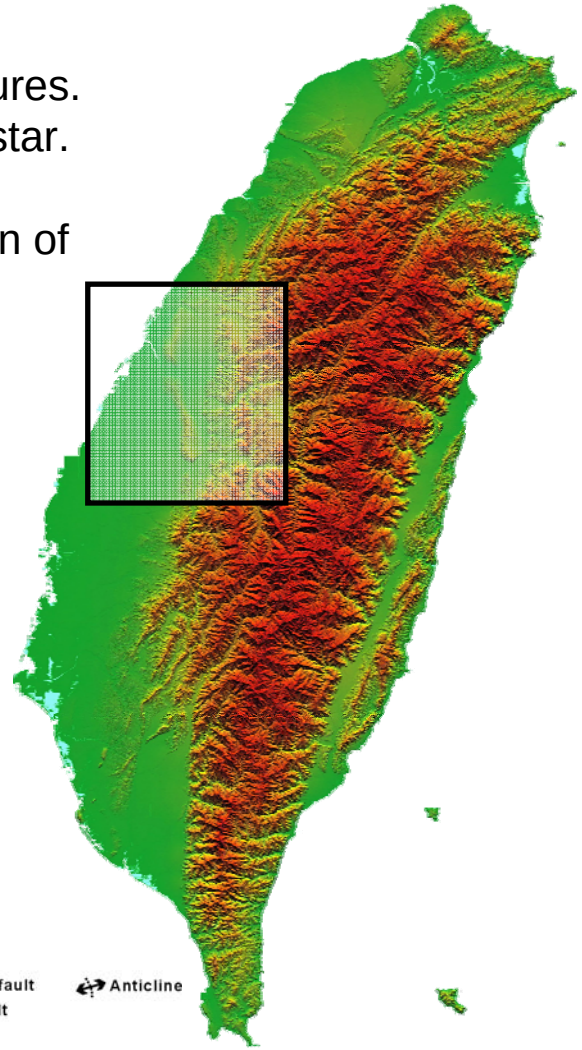

Main shock
Chelungpu fault
STF Shuangtung fault
CHF Chanhua fault
Anticline

N ⟷ S

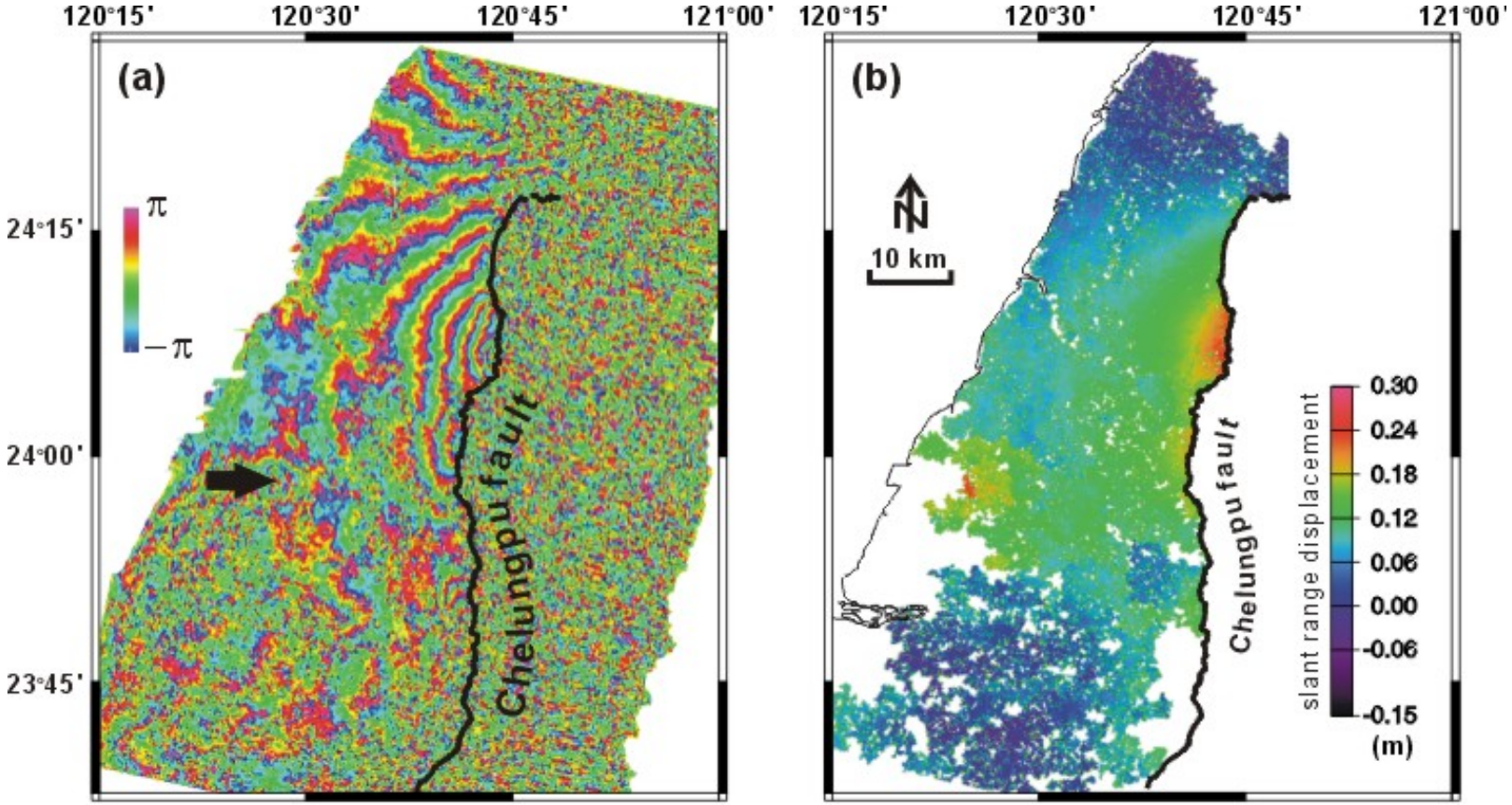

(a) Interferogram of the central Taiwan area (1999/5/6~1999/10/28; year/month/day).

(b) Unwrapped result of interferogram. The amount of displacement is evaluated in slant range direction.

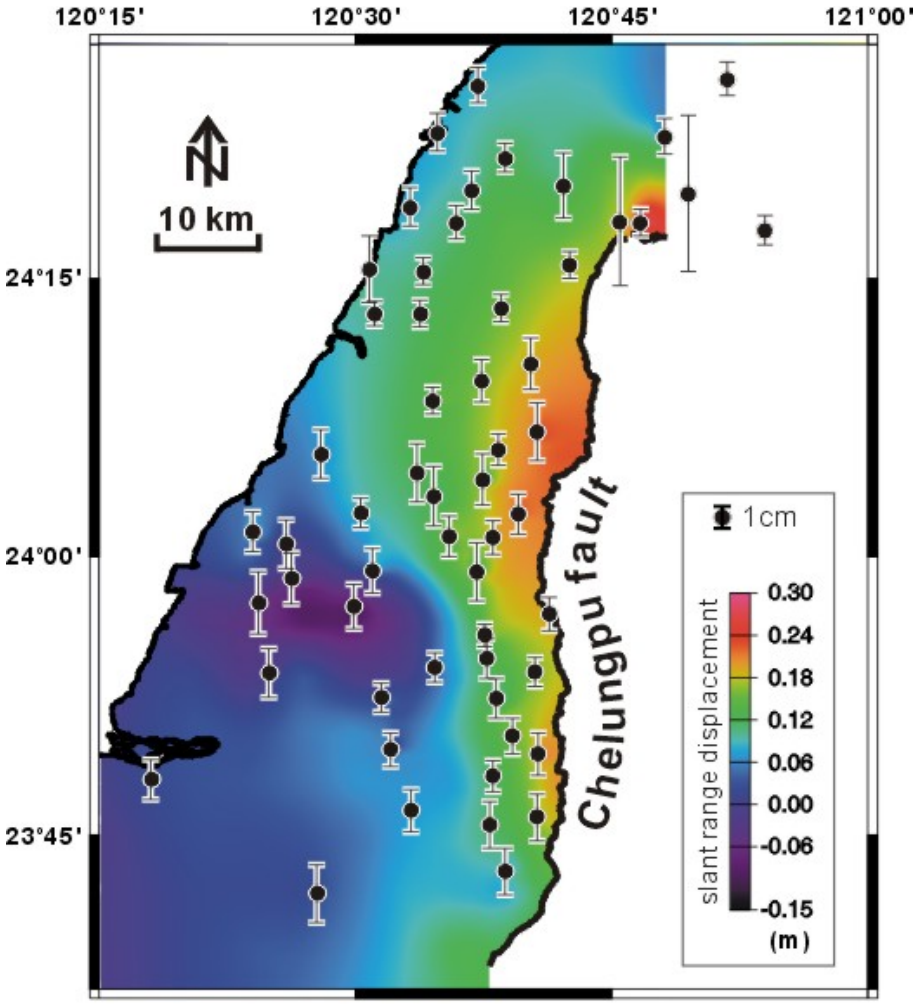

1. To simulate the interferogram of the C-band radar image, we projected each GPS displacement vector onto the slant range direction.
2. The GPS data used in this study were collected from several campaigns mainly conducted by (1) the Central Geological Survey, Ministry of Economic Affairs, (2) the Satellite Survey Division and Land Survey Bureau, Ministry of Interior, and (3) the Institute of Earth Sciences, Academia Sinica.
3. The GPS measurements were collected within 2~32 months before and 3 months after the mainshock of the Chichi earthquake.

Near-field co-seismic slant range displacement estimated from GPS measurements. Error bar (95% confidence) in slant range has been added on each station (data after Yu *et al.* 2001). Note that the color code used is the same as that in the figure before.

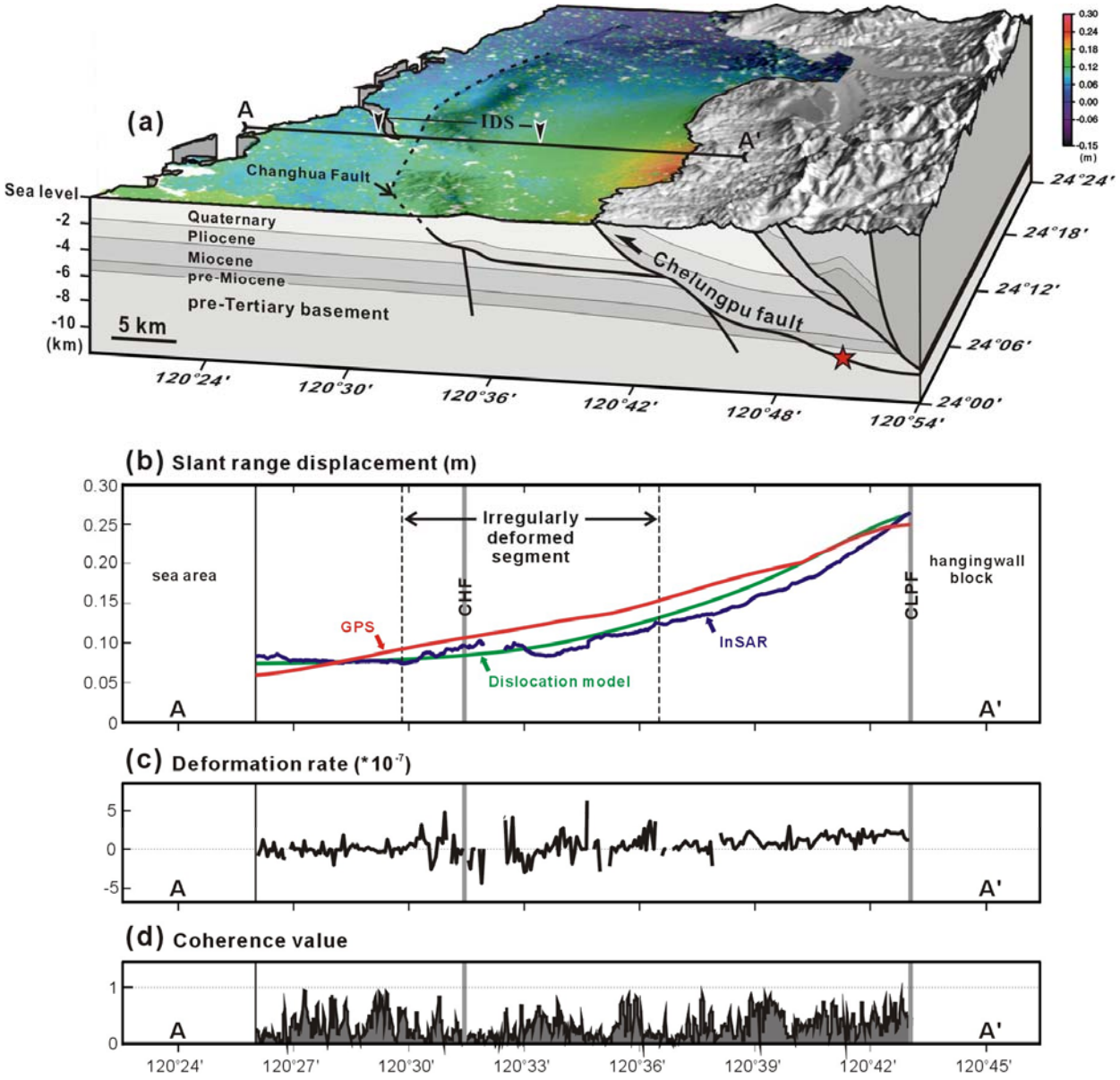

a. Block diagram showing the tectonic setting of the Taichung area. The unwrapped interferogram is overlaid. The epicenter of the mainshock is shown as a red star.

b. Slant range displacement along Profile AA' derived from different approaches. The blue line represents the measurements from the InSAR method; the red line represents the GPS measurements; and the green line shows the displacement synthesized using the elastic dislocation model.

c. The deformation gradient of Profile AA' evaluated from the InSAR observations.

d. The coherence of the images used along Profile AA'.

2. Tectonic uplift of Tainan area (southwestern Taiwan)

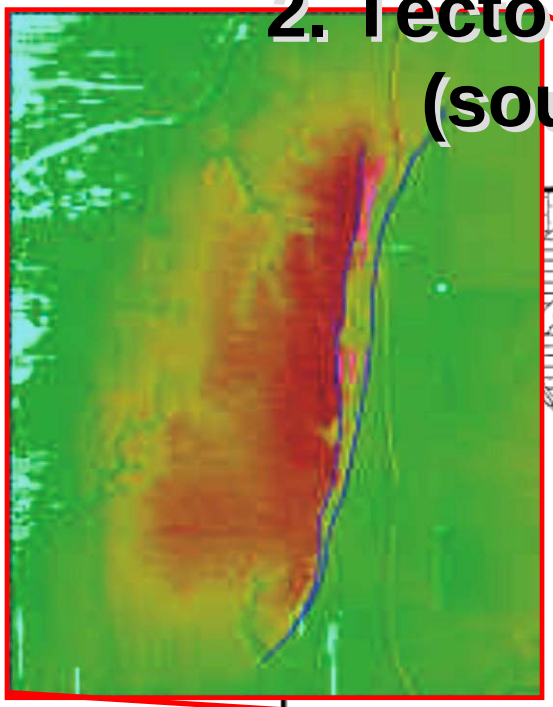

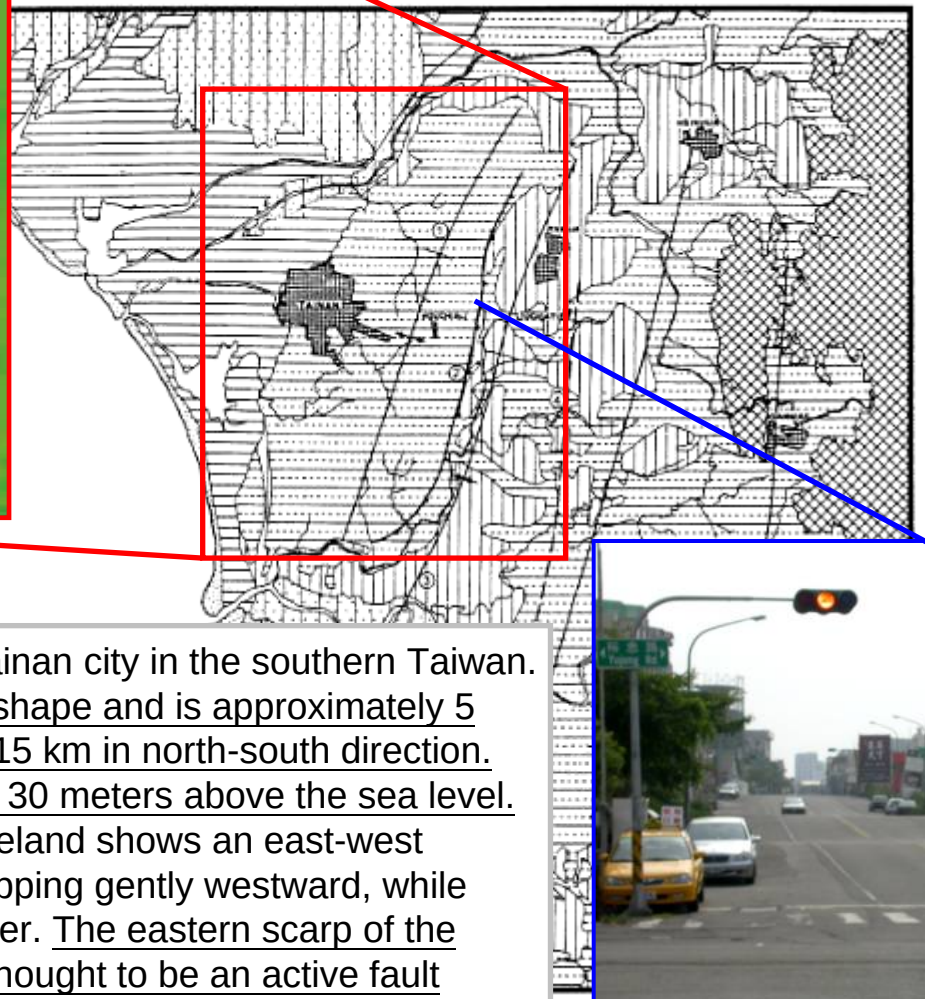

Tainan tableland surrounds Tainan city in the southern Taiwan. This tableland is elongated in shape and is approximately 5 km in east-west direction and 15 km in north-south direction. Its maximum altitude achieves 30 meters above the sea level. The topography of Tainan tableland shows an east-west asymmetry, its western part dipping gently westward, while the eastern part is being steeper. The eastern scarp of the Tainan tableland is generally thought to be an active fault (named as Houjiali fault; Sun, 1964; Chang et al., 1998).

Interferograms of the Tainan area

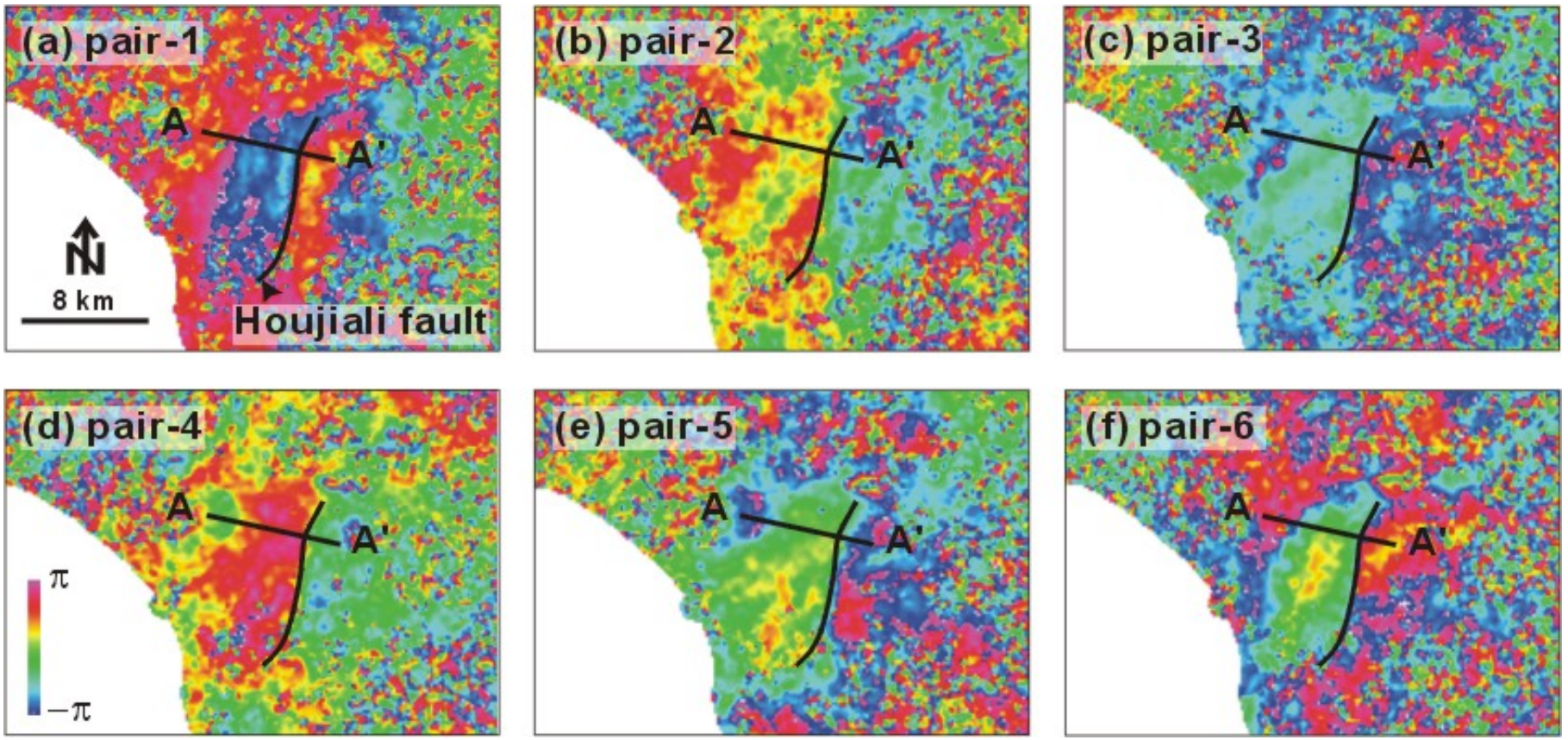

(a) Pair-1: 1997/2/20~1998/2/5 (year/month/day); (b) Pair-2: 1998/1/1~1998/11/12; (c) Pair-3: 1998/1/1~1999/1/21; (d) Pair-4: 1998/11/12~2000/1/6; (e) Pair-5: 1999/1/21~2000/1/6; (f) Pair-6: 2000/1/6~2000/11/16.

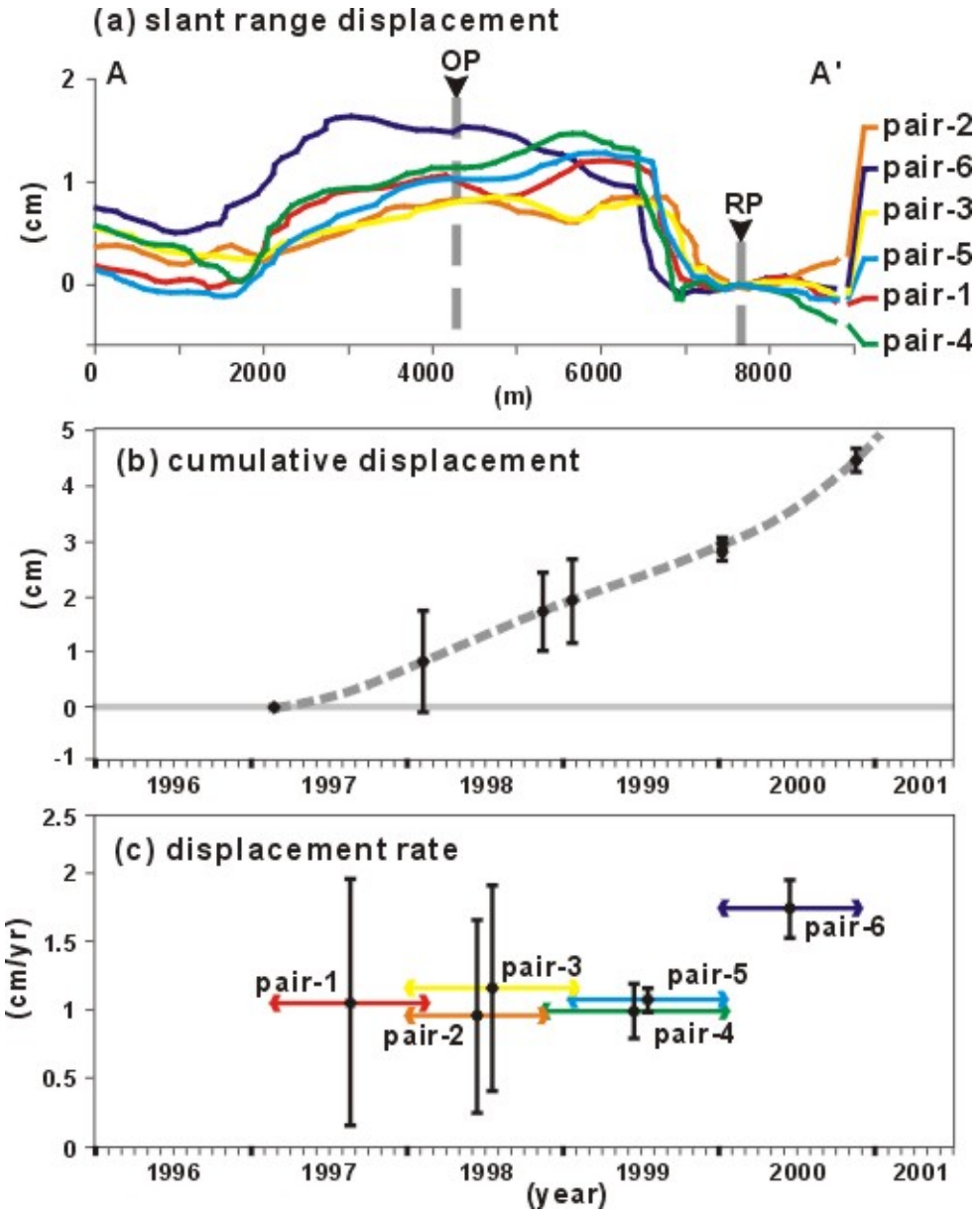

(a) Slant range displacement along the profile AA'. **OP**: observing point; **RP**: reference point.

(b) Estimated cumulative displacement between **OP** and **RP** in Figure a. Error bar is estimated from the ratio of the topographic altitude (*ht*) to the altitude of ambiguity (*ha* ~ 9416/vertical baseline offset) (error = wave length * *ht* / *ha*).

(c) Displacement rate between the **OP** and **RP** of each image pairs in Figure a.

3. Active deformation of the Hukuo area (northwestern Taiwan)

The Hukou fault (also called as the Yangmei fault) is the most important east-west striking structure in the northwestern Taiwan. The linear scarp of this fault is clear; however, no outcrop has been found along this lineament. The existence of this fault and whether the fault is active has been in debate. After considering the stratigraphic features, some geologists believed that the regional deformation may be controlled by an active fold – the Hukou anticline.

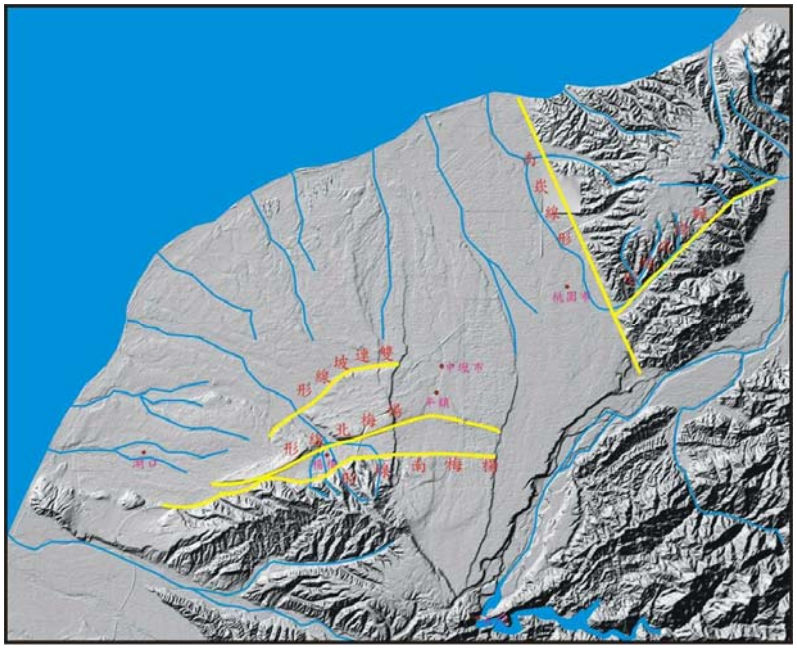

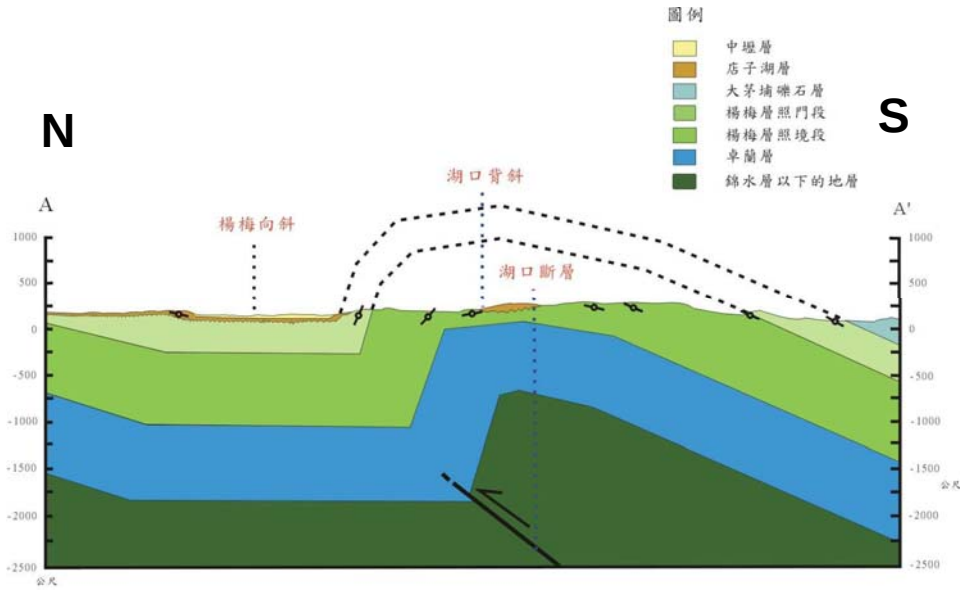

(data after CGS)

Interferograms of the Hukou area

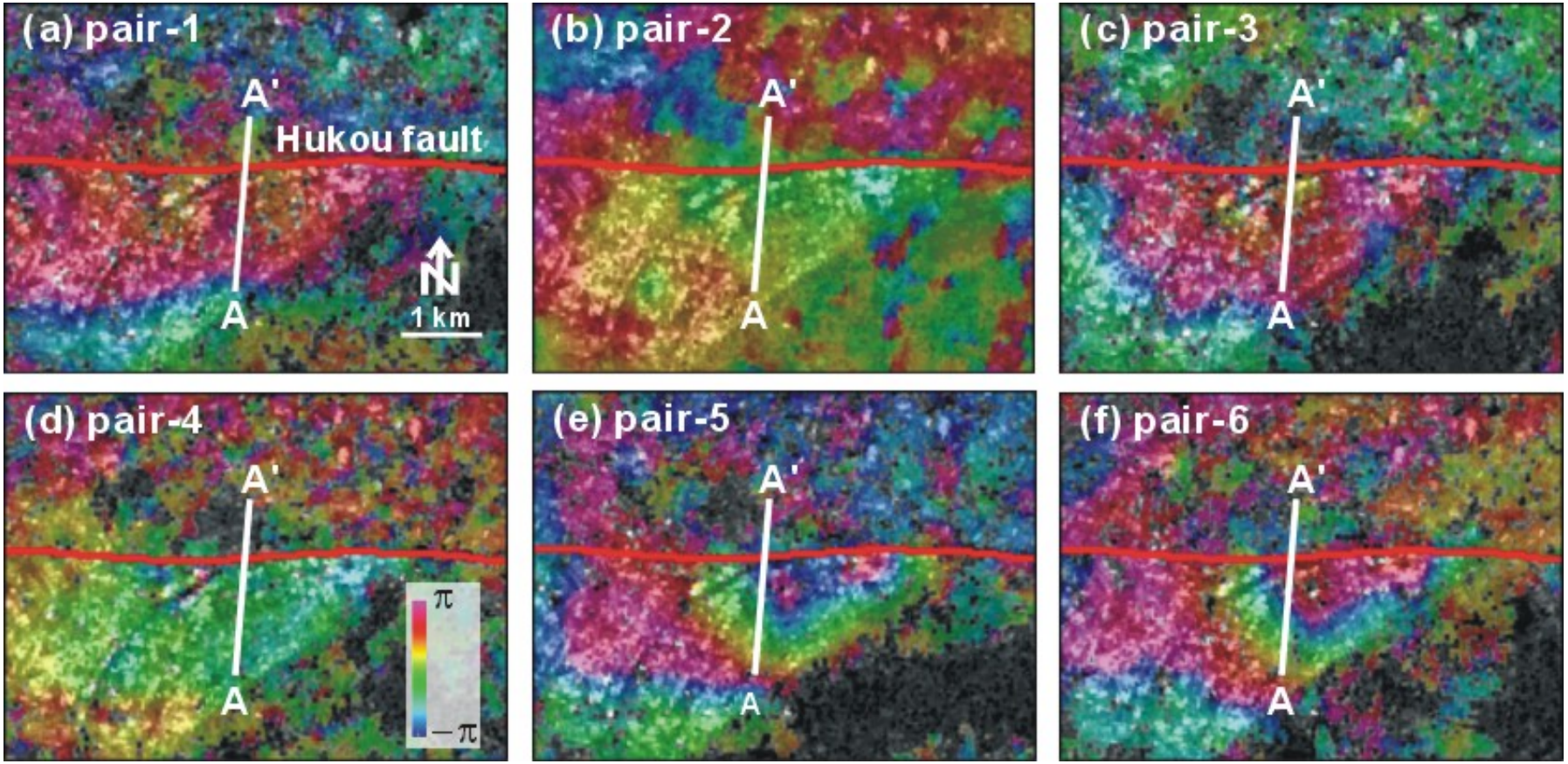

(a) Pair-1: 1993/11/10~1995/6/16 (year/month/day); (b) Pair-2: 1996/1/12~2000/1/22; (c) Pair-3: 1997/2/1~1999/7/31; (d) Pair-4: 1998/3/28~2000/1/22; (e) Pair-5: 2000/1/22~2003/2/15; (f) Pair-6: 2000/8/19~2003/2/15.

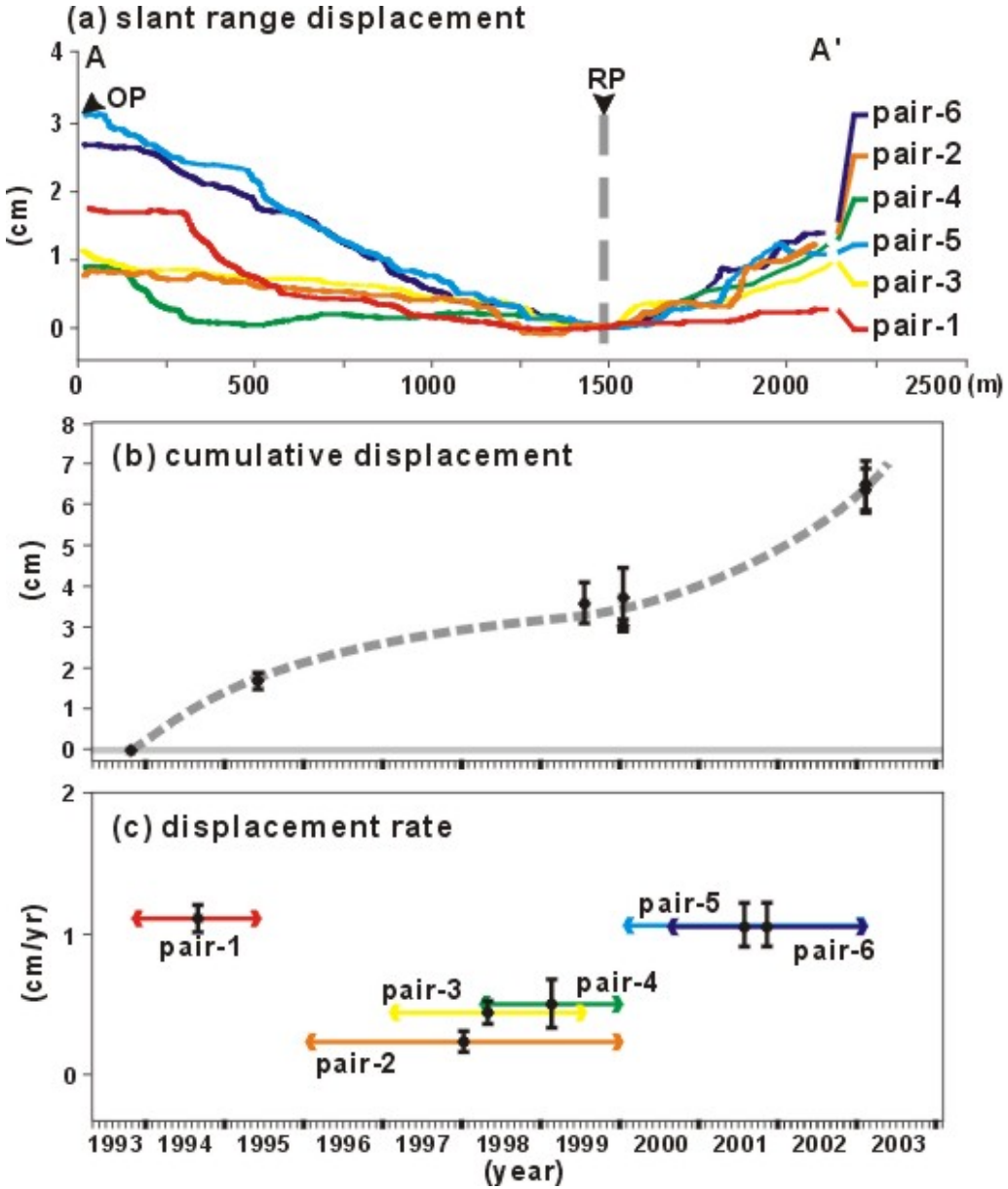

(a) Slant range displacement along the profile AA'. **OP**: observing point; **RP**: reference point.

(b) Estimated cumulative displacement between **OP** and **RP** in Figure a. Error bar is estimated from the ratio of the topographic altitude (*ht*) to the altitude of ambiguity (*ha* ~ 9416/vertical baseline offset) (error = wave length * *ht* / *ha*).

(c) Displacement rate between the **OP** and **RP** of each image pairs in Figure a.

4. Rapid land-subsidence of the Chungli area (northern Taiwan)

The crustal deformation caused by human activity is generally very local, unsteady, and cannot be explained by regional tectonic regimes or local structural geology. Since these deformations are mostly temporal, of which the deformation rate and style may change very rapidly. All these make the measurement of surface deformation a difficult task. Moreover, human activity is concentrated in urban areas, where cover and shadow from buildings raise errors in GPS observation.

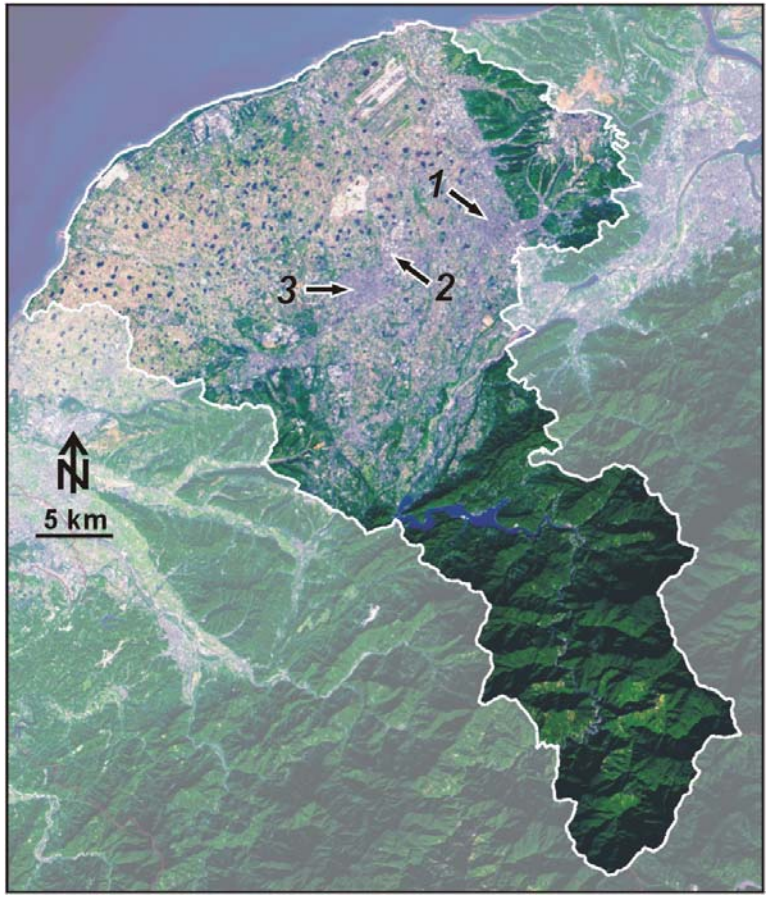

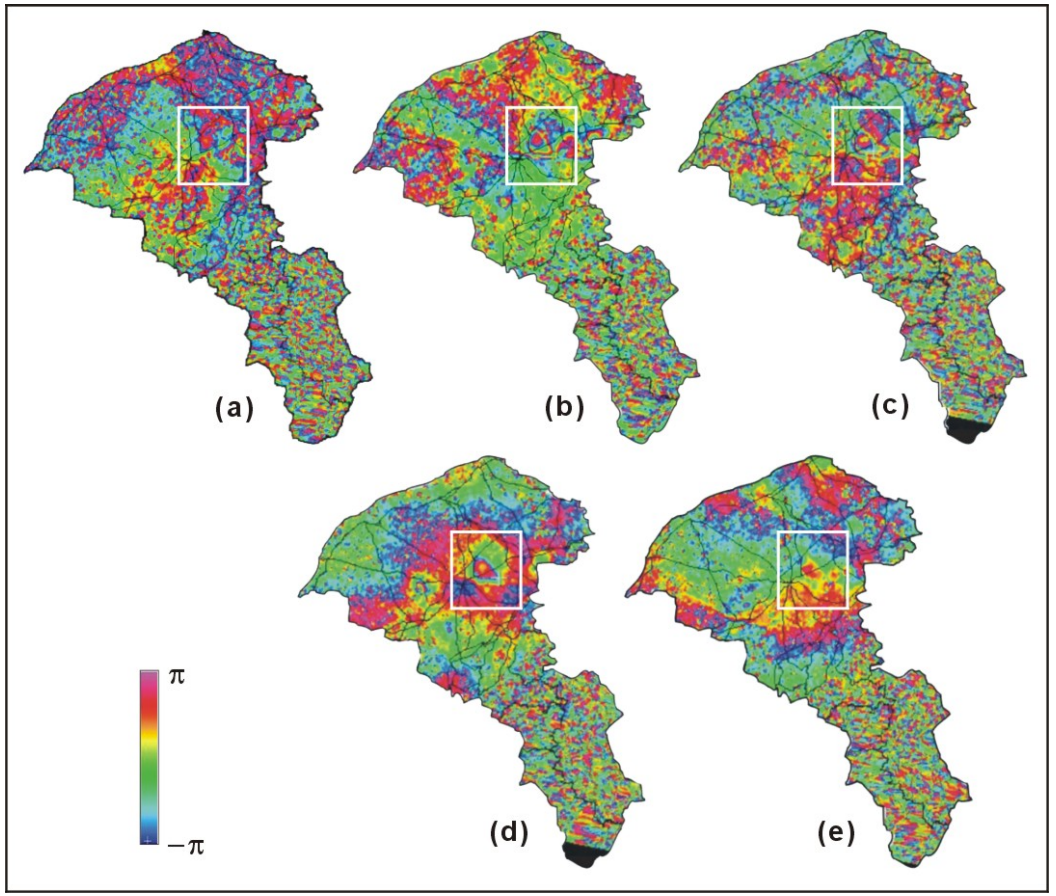

Interferograms of the Chungli area

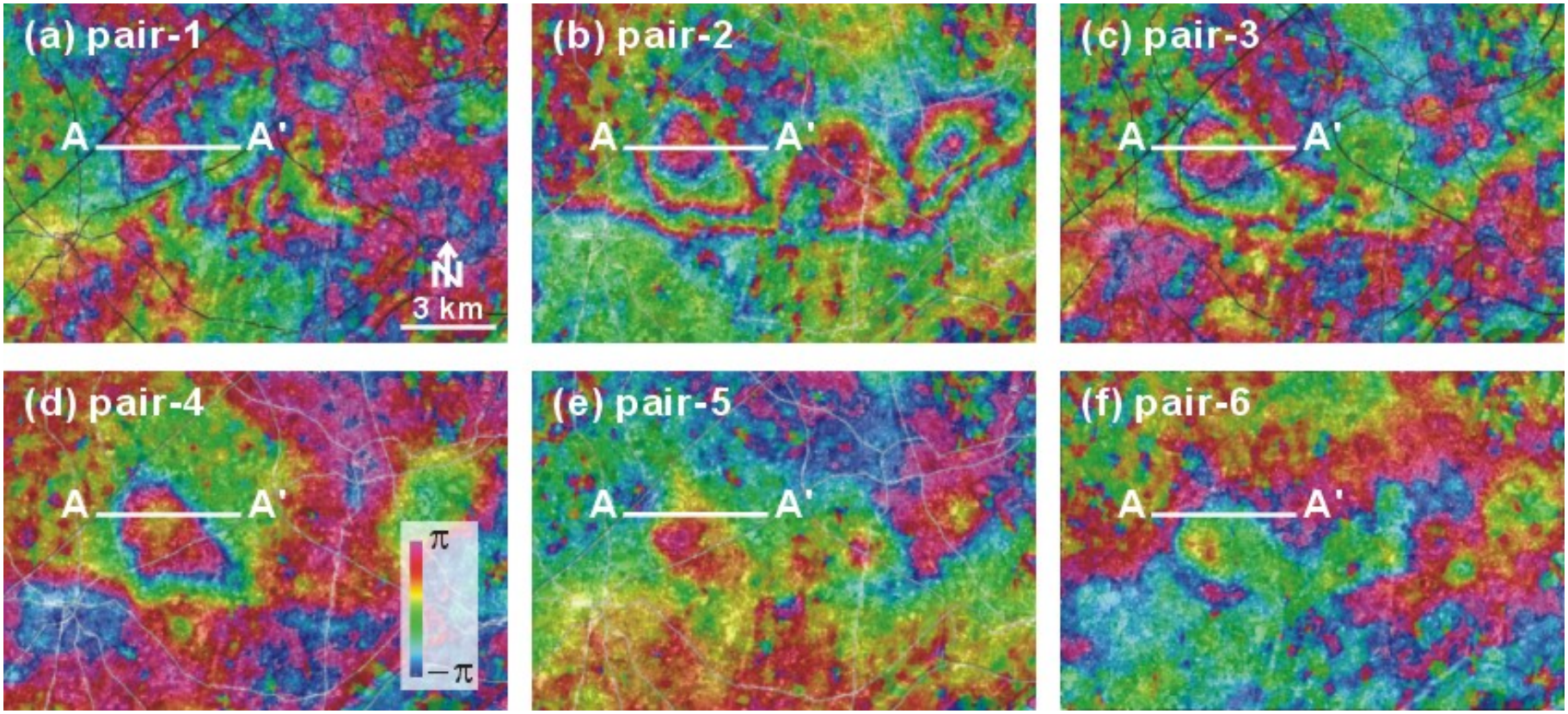

(a) Pair-1: 1993/11/10~1995/6/16 (year/month/day); (b) Pair-2: 1996/1/12~2000/1/22; (c) Pair-3: 1997/2/1~1999/7/31; (d) Pair-4: 1998/3/28~2000/1/22; (e) Pair-5: 2000/1/22~2003/2/15; (f) Pair-6: 2000/8/19~2003/2/15.

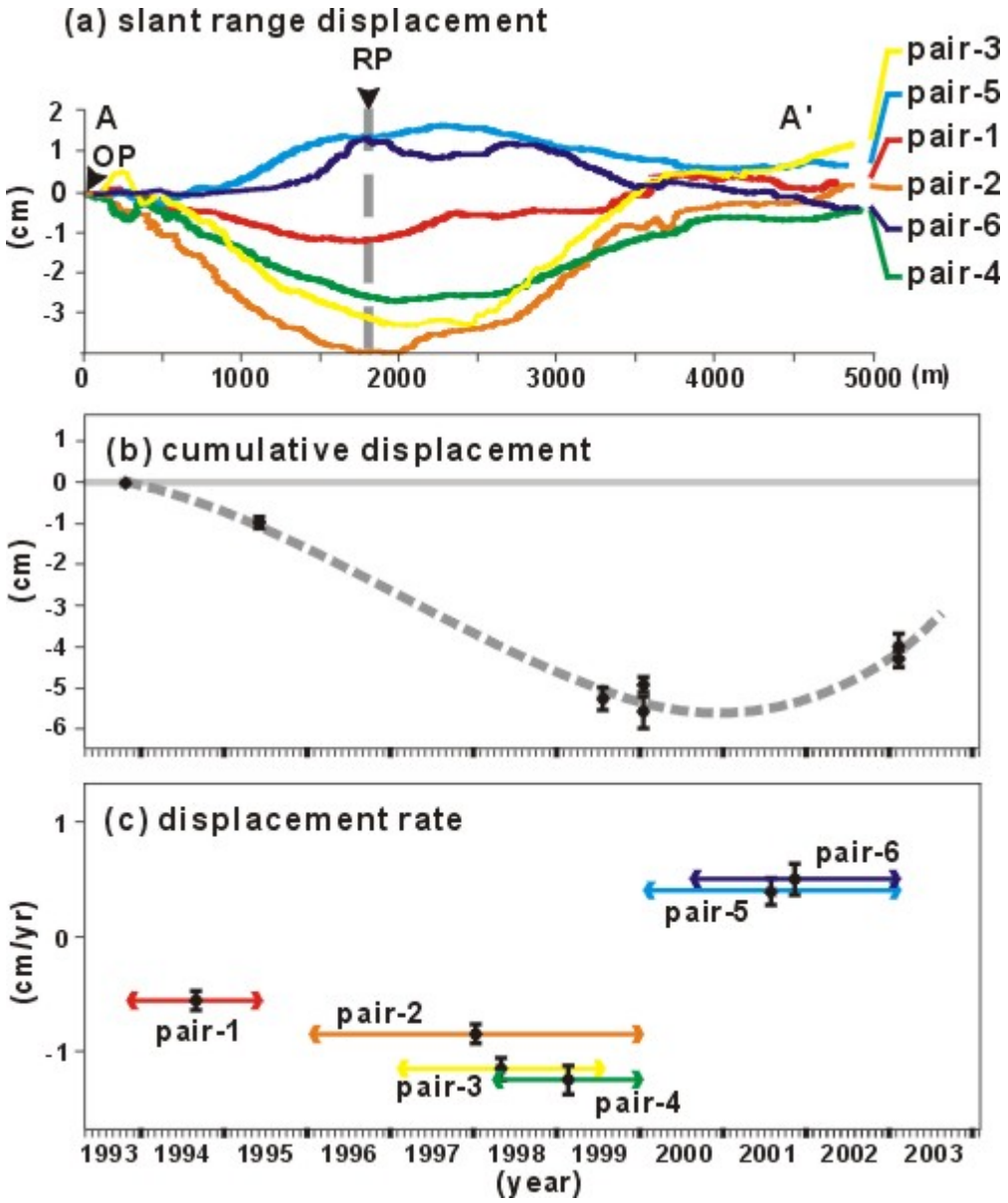

(a) Slant range displacement along the profile AA'. **OP**: observing point; **RP**: reference point.

(b) Estimated cumulative displacement between **OP** and **RP** in Figure a. Error bar is estimated from the ratio of the topographic altitude (*ht*) to the altitude of ambiguity (*ha* ~ 9416/vertical baseline offset) (error = wave length * *ht* / *ha*).

(c) Displacement rate between the **OP** and **RP** of each image pairs in Figure a.

5. seasonal-varied land-subsidence in the Pingtung area (southern Taiwan)

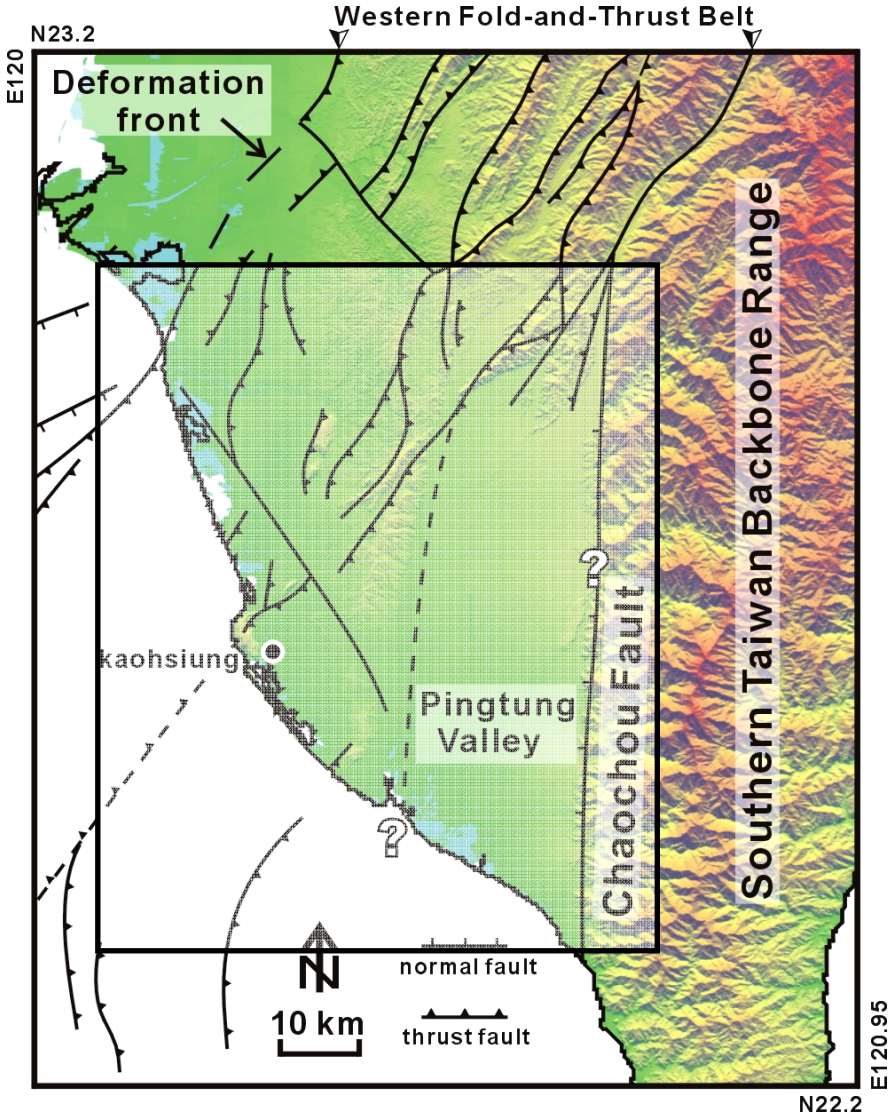

The Pingtung plain is elongated in shape with an area of 1,210km2, roughly 55km in length and 20km in width. The highest elevation point on this plain is 80m above the mean sea level, located in its northeastern most corner, which means the plain dips on a very gentle gradient to the southwest. The entire Pingtung plain is composed of fluvial gravel and sand in the top several tens of meters. In general, grain size decreases from east to west as well as from north to south.

Tectonic setting of the Pingtungn plain. Tentative structural model of escaping blocks in SW Taiwan (modified after Lacombe et al., 2001).

Daily rainfall of the Kaohsiung station

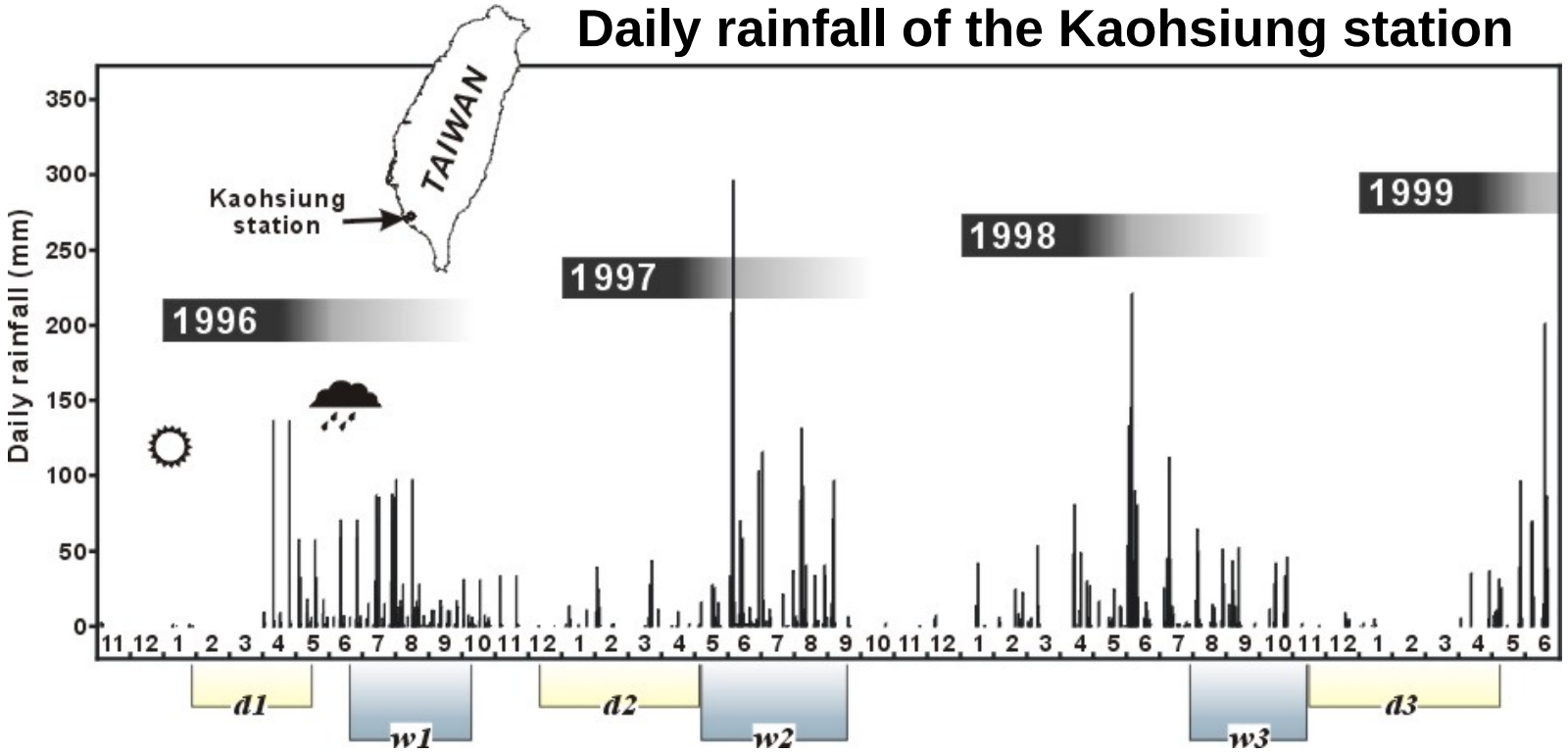

Pair	Master image	Slave image	$B_{//}$ (m)	$B_{\perp}$ (m)	Days
d1	1996.01.31	1996.05.16	57	0	106
d2	1996.12.12	1997.05.01	-25	34	140
d3	1998.11.12	1999.05.06	-55	-92	175
w1	1996.06.20	1996.10.03	10	21	105
w2	1997.05.01	1997.09.18	57	90	140
w3	1998.07.30	1998.11.12	-56	-92	175

(Track = 232, Frame = 3141)

Parameters of the ERS2-SAR images used in this study

Date of acquisition, interval time, vertical baseline offset, and parallel baseline offset are shown.

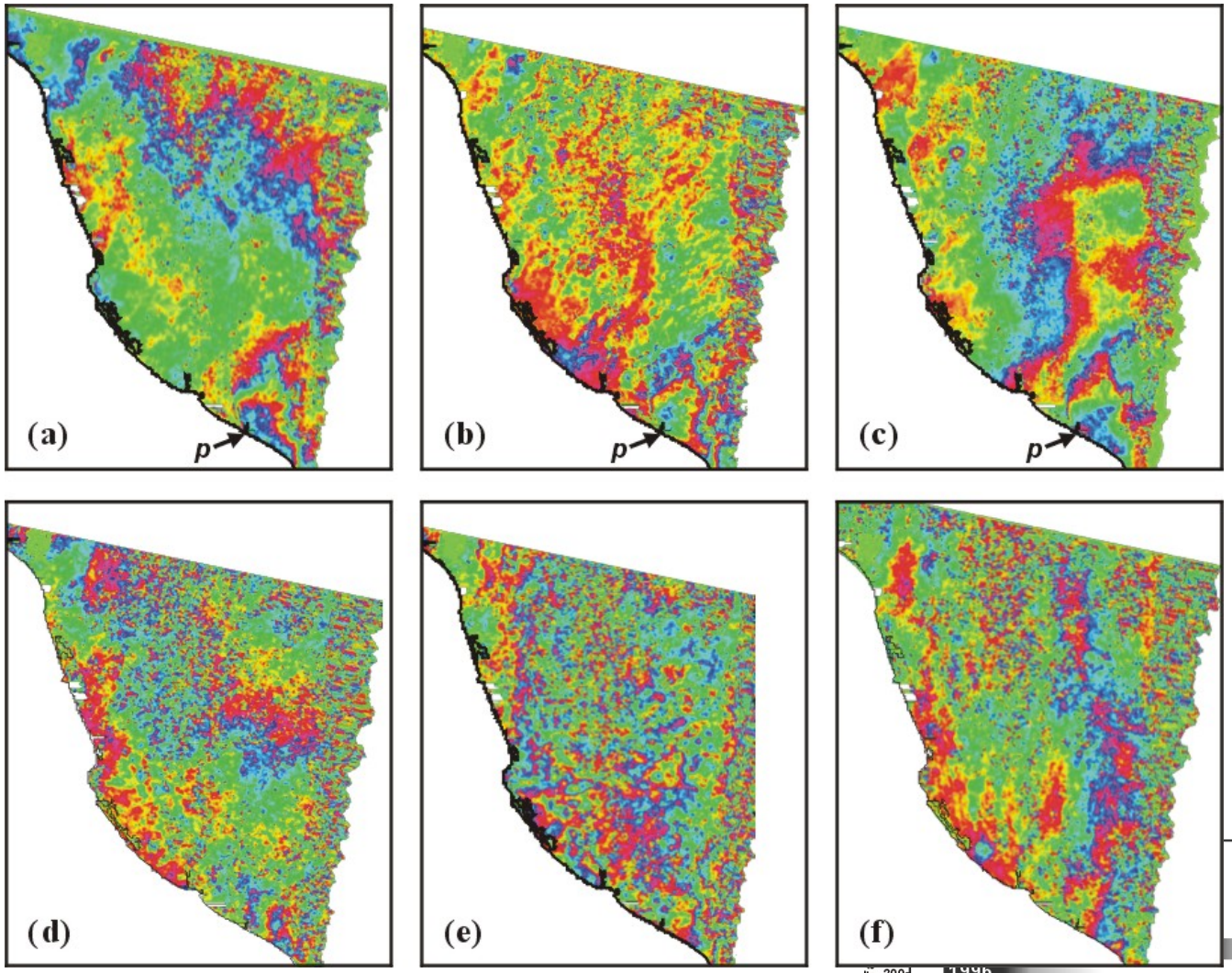

Dry season

Wet season

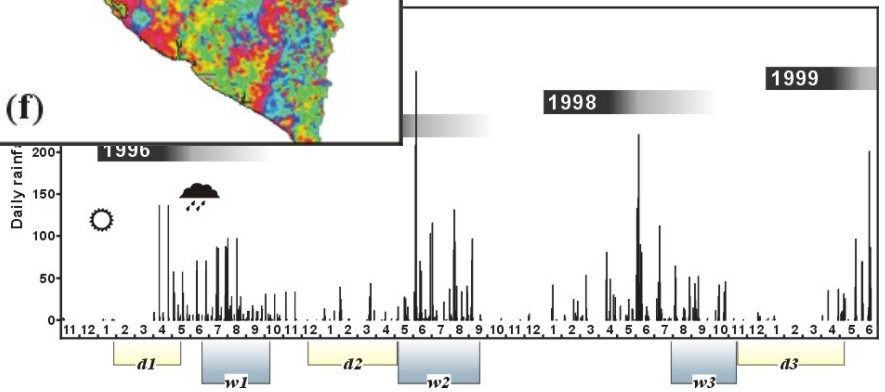

Resulted differential interferograms of different season

N
S

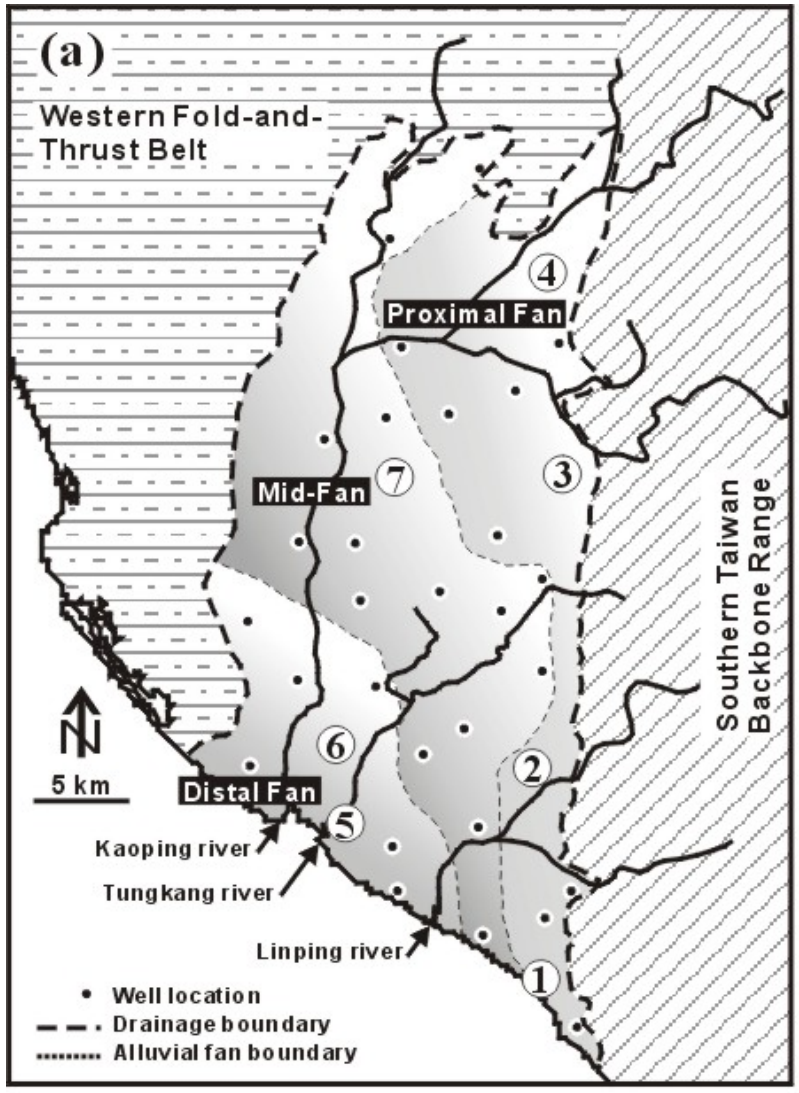

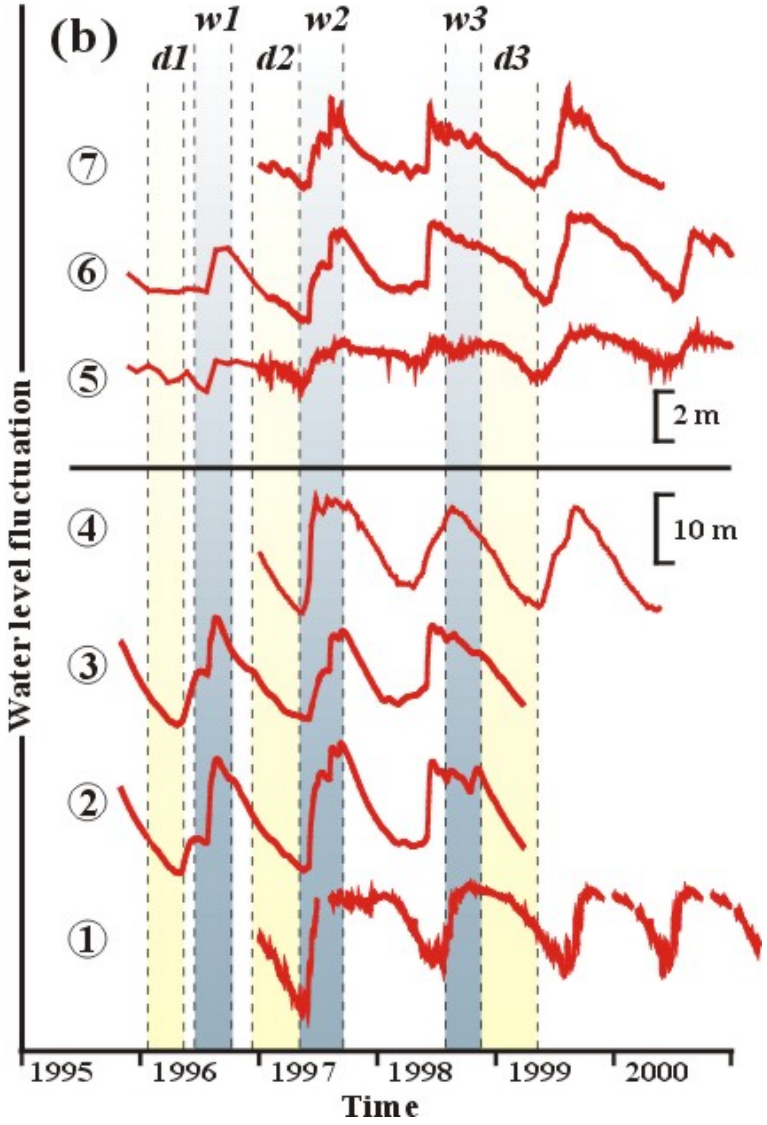

Groundwater level fluctuations of the Pingtung plain

Conclusion

1. In the case of intense event, concentric fringe patterns clearly indicate the co-seismic deformation in the Taichung area. In gentle event cases, the Tainan and Hukou areas show a continuous tectonic deformation. The Chungli and Pingtung areas show a rate-changed subsidence induced by water pumping activity.

2. The application of radar interferometry presented in this study shows that, with suitable images, this technique is a useful high-resolution tool for monitoring different types of crustal deformation in spite of the difficulties proposed due to dense subtropical vegetation in an area such as Taiwan.

3. According to the cases presented in this paper, areas with high deformation rates are all next to highly populated areas or industrial parks. To mitigate potential hazards, continuous monitoring and further study of neo-tectonics and human activities are urgently needed. We believe that geological applications for radar interferometry and other space geodetic tools will continue to grow rapidly.

This work is principally supported by Central Geological Survey (grant no. 5226902000 -03-93-04), National Science Council (grant no. NSC92-2119-M-008-016), and the Ministry of Education (grant no. 91-N-FA07-7-4).

ERS-2 satellite Cite de l'Espace, Toulouse, France